energies

MDPI

Article

Performance Analysis of Vermiculite–Potassium Carbonate Composite Materials for Efficient Thermochemical Energy Storage

Jianquan Lin [1,*], Qian Zhao [1,*] and Haotian Huang [2]

[1] Urban Construction College, Changzhou University, Changzhou 213164, China
[2] Shanghai Institute of Optics and Fine Mechanics, Chinese Academy of Sciences, Shanghai 201899, China; huanghaotian@siom.ac.cn
* Correspondence: linjianquan@cczu.edu.cn (J.L.); zhaoqian@cczu.edu.cn (Q.Z.)

Abstract: In this study, the preparation of the composite material consisting of expanded vermiculite (EV) and potassium carbonate (K_2CO_3) was conducted using a solution impregnation method. Sorption and desorption experiments were undertaken to investigate the dynamic and thermodynamic properties of the EV/K_2CO_3 composites with varying salt contents. The findings suggest that the EV/K_2CO_3 composites effectively address the issues of solution leakage resulting from the deliquescence and excessive hydration of pure K_2CO_3 salt, thereby substantially improving the water sorption capacity and overall stability of the composite materials. The salt content plays a vital role in the sorption and desorption processes of EV/K_2CO_3 composites. As the salt content rises, the resistance to sorption mass transfer increases, resulting in a decline in the average sorption rate. Concurrently, as the salt content increases, there is a corresponding increase in the average desorption rate, water uptake, and heat storage density. Specifically, at a temperature of 30 °C and a relative humidity of 60%, the $EVPC_{40}$ composite with a salt content of 67.4% demonstrates water uptake, mass energy density, and volumetric energy density values of 0.68 g/g, 1633.6 kJ/kg, and 160 kWh/m^3, respectively. In comparison to pure K_2CO_3 salt, the utilization of EV/K_2CO_3 composites under identical heat demand conditions results in a 57% reduction in the required reaction material. This study offers essential empirical evidence and theoretical backing for the utilization and development of EV/K_2CO_3 composites within thermochemical energy storage systems.

Keywords: potassium carbonate; expanded vermiculite; composite material; salt content; thermochemical energy storage

check for updates

Citation: Lin, J.; Zhao, Q.; Huang, H. Performance Analysis of Vermiculite–Potassium Carbonate Composite Materials for Efficient Thermochemical Energy Storage. *Energies* **2024**, *17*, 2847. https://doi.org/10.3390/en17122847

Academic Editor: Fabio Montagnaro

Received: 30 April 2024
Revised: 31 May 2024
Accepted: 6 June 2024
Published: 9 June 2024

Copyright: © 2024 by the authors. Licensee MDPI, Basel, Switzerland. This article is an open access article distributed under the terms and conditions of the Creative Commons Attribution (CC BY) license (https://creativecommons.org/licenses/by/4.0/).

1. Introduction

Due to the persistent expansion of the population, economic development, and worsening environmental conditions, conventional fossil fuels have become inadequate for satisfying the escalating energy requirements of contemporary society [1]. The exploration of renewable energy sources and the implementation of energy efficiency policies pave a way forward for future energy systems. Solar energy is a cheap and clean renewable energy source that is abundant and may be widely used for building space heating and domestic hot water supply [2]. However, the intermittent and fluctuating nature of solar energy poses a major challenge for its effective storage and utilization [3–6]. The thermochemical energy storage (TCES) system is an emerging technology with wide application prospects [7–10]. It may be used to solve the mismatch between energy supply and demand in time, space, and intensity. As such, it may contribute to improving the comprehensive utilization rate of renewable energy and promote the process of energy decarbonization.

In recent years, the low-temperature TCES technology utilizing inorganic salt/water working pairs has garnered significant attention for residential building heating demand [11–13]. Notably, chloride, sulfate, and bromide salts have been extensively investigated as hydrated

salts. Nevertheless, it is important to acknowledge that each of these materials presents distinct limitations [14]. Chloride salts offer low cost and wide applicability but exhibit low thermal conductivity and poor reaction stability. Sulfate salts boast higher energy density but suffer from slow reaction rates and low hydration temperatures. Strontium bromide, despite its advantageous stability and elevated thermal efficiency, presents potential contact hazards and is associated with substantial expenses. Donkers et al. [15] collected and analyzed thermodynamic data from 574 hydrated salt reactions. Through the application of filtering criteria, they ultimately identified 25 suitable hydrated salts meeting the requirements for space heating, with potassium carbonate (K_2CO_3) being considered the most promising candidate for TCES system development.

K_2CO_3, a low-temperature thermochemical material (TCM), exhibits notable safety characteristics and minimal corrosiveness, while also being cost-effective at approximately 6500 RMB/ton. Moreover, the hydration/dehydration process of K_2CO_3 is straightforward, involving a single-step transformation between anhydrous K_2CO_3 and $K_2CO_3 \cdot 1.5H_2O$ [16,17]. When subjected to operating conditions of 20 mbar/65 °C for dehydration and 12 mbar/59 °C for hydration, the material-level energy densities of K_2CO_3 in open and closed systems are 1.3 GJ/m^3 and 0.96 GJ/m^3, respectively [18]. However, the application of K_2CO_3 in practical TCES systems may encounter challenges, such as slow hydration rates, expansion and contraction, particle aggregation, and deliquescence, due to changes in operating conditions [19]. To tackle these concerns, a promising strategy involves employing porous matrices, capitalizing on their porous characteristics to disperse salt particles and accommodate salt solutions, thereby averting leakage during excessive water sorption and deliquescence.

Silica gel and zeolite are commonly recognized as porous materials that enhance water sorption performance. Expanded graphite is known for its commendable thermal conductivity, while activated carbon exhibits a high porosity. Recently, expanded vermiculite (EV) has attracted significant attention due to its substantial pore volume and high porosity. Consequently, it has been extensively utilized in composite material performance testing, often in conjunction with various salt hydrates. Aydin et al. [20] conducted an evaluation of the performance of EV/$CaCl_2$ and zeolite 13X/$CaCl_2$ composite materials, revealing the superior cyclic and reactive properties of EV/$CaCl_2$. Casey et al. [21] examined samples with silica gel, zeolite, and EV as matrix materials matched with five salt hydrates, ultimately concluding that EV demonstrated a more stable structure as a matrix material. Zhang et al. [22] investigated EV/LiCl composite materials, suggesting enhanced mass transfer capability and thermochemical performance in comparison to pure LiCl salt. Furthermore, Zhang et al. [23] conducted an investigation of the thermochemical performance of EV/$SrBr_2$ composite materials. Their findings revealed that the inclusion of EV could accommodate excess hydrated $SrBr_2$ solution, thereby improving the stability and energy storage density of the composite material. This was substantiated through thermochemical assessments conducted on EV/$CaCl_2$ composite materials. These studies collectively indicate that EV possesses a high level of dispersibility and a significant capacity to accommodate salt solutions. These properties effectively mitigate material agglomeration and solution loss that may occur during the reaction process. Due to its large pore volume and high porosity, EV-based composite sorbents demonstrate elevated liquid-holding capacities while retaining superior cycling properties, chemical stability, and thermal stability. Consequently, EV is a suitable candidate for pairing with hydrates that are susceptible to volume changes and deliquescence, making it a promising matrix material option for K_2CO_3.

Zou et al. [24] employed various preparation methods to fabricate EV/K_2CO_3 composite materials, revealing that the vacuum degree and particle size of EV have the potential to modify the microstructure of the composite material, thereby affecting its density and salt content. Fisher et al. [25] successfully synthesized EV/K_2CO_3 composite materials with a salt content of 33.85%, thereby showcasing enhanced water sorption capabilities and reaction rate in comparison to pure K_2CO_3 salt. Shkatulov et al. [26] effectively developed EV/K_2CO_3 composite materials containing a salt content of approximately 69%. The com-

posite materials demonstrated enhanced hydration rates compared to pure K_2CO_3 salt and exhibited stable performance for 47 cycles under deliquescence conditions. These findings suggest that the utilization of EV as a matrix material can mitigate certain obstacles related to sluggish hydration rates and particle aggregation in pure K_2CO_3 salt.

Currently, there is a dearth of research on the thermochemical properties of EV/K_2CO_3 composite materials in the academic literature. Existing studies primarily concentrate on the characterization of morphology and performance evaluation of composite materials under specific salt content conditions. Nevertheless, it is crucial to recognize that the salt content has a significant impact on the microstructure and water sorption capabilities of the composite materials, consequently influencing their reaction rate and thermal energy storage capacity. Therefore, it is imperative to conduct investigations into the performance of composite materials under varying salt contents. In this study, EV/K_2CO_3 composite materials with different salt contents were fabricated. The microstructure of each sample was analyzed utilizing scanning electron microscope (SEM), and the sorption and desorption properties of EV/K_2CO_3 composite materials with different salt contents were investigated through sorption and desorption experiments conducted in a constant temperature and humidity chamber (CTHC) and using thermogravimetry (TG). Based on these premises, the primary thermodynamic parameters, namely mass energy storage density (MESD) and volumetric energy storage density (VESD), of EV/K_2CO_3 composite materials were evaluated utilizing the test outcomes obtained from differential scanning calorimetry (DSC). The objective was to furnish fundamental data and theoretical backing for the design and implementation of EV/K_2CO_3 composite materials within TCES systems.

2. Materials and Methods

2.1. Preparation of Composite Materials

EV/K_2CO_3 composites were prepared using the solution impregnation method. Anhydrous K_2CO_3 salt of analytical purity (99.9%) was procured from Chengdu Chron Chemical Co., Ltd. (Chengdu, China), while EV was sourced from Hebei Lingshou (Shijiazhuang, China). The preparation procedure encompassed four primary steps, namely drying of EV and preparation of K_2CO_3 solution, impregnation of EV with K_2CO_3 solution, filtration, and subsequent drying of the EV/K_2CO_3 composites. The entire procedure is illustrated in Figure 1. Firstly, K_2CO_3 solutions with mass concentrations of 10%, 20%, 30%, and 40% were prepared separately using anhydrous K_2CO_3 salt and distilled water. The solutions were stirred with an ultrasonic stirrer for 5 min to ensure thorough mixing of the solvent and solute, followed by cooling to room temperature (approximately 28 °C). EV with a particle size of 2–4 mm was chosen as the porous substrate and dried in a vacuum oven at 200 °C for 12 h to eliminate any moisture adsorbed in the EV pores. Subsequently, the dried EV was immersed in the prepared K_2CO_3 solutions for 72 h to ensure complete saturation of the EV pores with the K_2CO_3 solutions. The wet EV/K_2CO_3 samples were then separated from the solutions using a sieve, and a quick rinse with distilled water was performed to remove any residual bonding solution from the surface. Finally, the wet EV/K_2CO_3 samples were thoroughly dried in a vacuum oven at 200 °C for 12 h, resulting in the formation of EV/K_2CO_3 composites. These composites were designated as $EVPC_{10}$, $EVPC_{20}$, $EVPC_{30}$, and $EVPC_{40}$, respectively, corresponding to the mass concentration of K_2CO_3 employed in the impregnation process.

2.2. Microscopic Characterization

The Helios Nanolab G3 SEM manufactured by FEI in the United States (Hillsboro, Oregon, USA) was utilized to conduct high-resolution microstructural analysis of EV/K_2CO_3 composites with different salt contents. In order to overcome the inadequate electrical conductivity of the EV/K_2CO_3 composites, the samples were coated with a layer of gold before testing. Subsequently, the gold-coated composite particles were placed on an aluminum table that was covered with double-sided adhesive carbon tape. The vacuum pressure within the

microscopy chamber was maintained at 3×10^{-5} mbar during the examination process, and SEM images were obtained using an electron beam with an acceleration voltage of 2 kV.

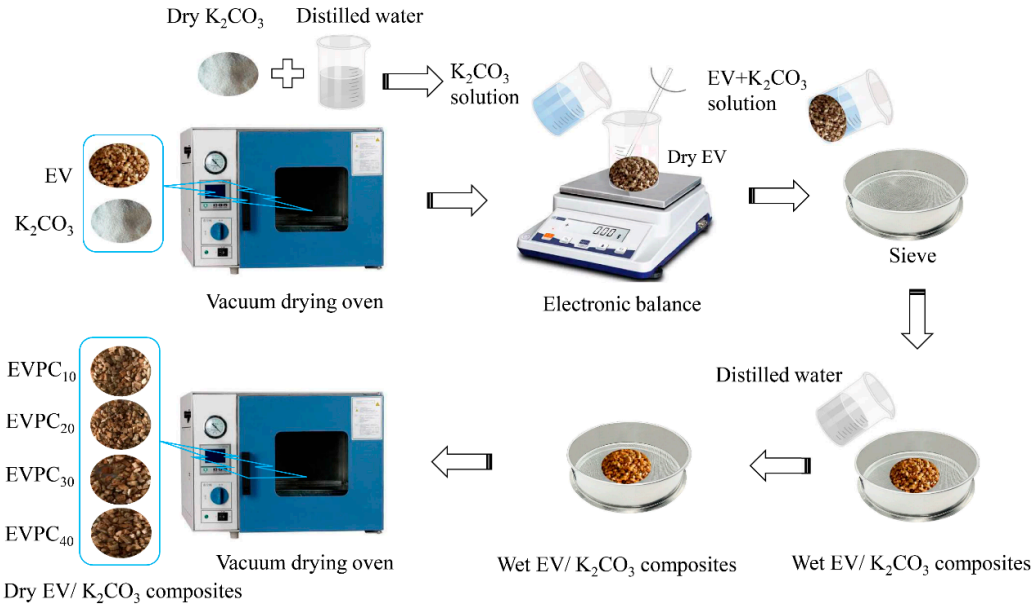

Figure 1. Preparation procedure of anhydrous EV/K_2CO_3 composites.

2.3. Sorption Experiments

Sorption experiments were performed on EV/K_2CO_3 composite materials with varying salt contents using a CTHC apparatus (TX-TH-150F, Dongguan Juya testing instrument equipment Co., Ltd., Dongguan, China) to determine the maximum allowable salt contents and the equilibrium sorption capacities achievable under specific operational parameters. For the CTHC, the measurement accuracies of the temperature and relative humidity (RH) are ±0.1 °C and ±2%, respectively. Considering an actual closed TCES system, the evaporation temperature is usually lower than 20 °C, and the sorption temperature is higher than 30 °C. Thus, 30 °C and 60% RH are considered to be the most unfavorable conditions (corresponding to an evaporation temperature of 20 °C) [23]. Therefore, 30 °C and 60% RH were applied as the experimental conditions for sorption in this study. The weight of each sample for the CTHC experiments was about 5 g. Before the experiment, samples were fully dried at 200 °C in a vacuum oven. Afterward, the dried samples were placed into the CTHC at the selected experimental temperature and RH. During the experiment, the mass variations of the samples were measured every half hour using an electronic balance with an accuracy of 0.001 g until the mass of the samples became constant. As it is well-known, the deliquescence relative humidity (DRH) of pure K_2CO_3 salt at room temperature is approximately 43% [27]. The propensity for deliquescence in pure K_2CO_3 salt occurs when the environmental RH surpasses this threshold, which should be avoided in TCES applications. Therefore, in order to examine the impact of RH on sorption performance, additional sorption experiments were conducted on the $EVPC_{40}$ sample under five distinct RH conditions (with a constant temperature of 30 °C): 29% RH, 40% RH, 44% RH, 55% RH, and 67% RH.

2.4. Desorption Experiments

Desorption experiments were conducted on EV/K_2CO_3 composite materials with varying salt contents utilizing a Simultaneous Thermal Analyzer (STA) Netzsch STA449 F3 (NETZSCH Group, Selb, Bavaria, Germany). This instrument allows for simultaneous measurements of TG and DSC, thereby facilitating the examination of both changes in mass and variations in heat flux during the desorption process. The resolutions of the measurements of mass and heat flux of the STA apparatus are 1 μg and 1 μW, respectively.

The measurement conditions were as follows: the weight of each sample for the STA test was about 10 mg, and the initial state was the sorption equilibrium state at 30 °C and 60% RH following the sorption experiment in the CTHC. The temperature ranged from room temperature (approximately 30 °C) to 250 °C at a heating rate of 10 K/min, and the purge gas was argon with a flow rate of 30 mL/min.

2.5. Cycle Experiments

The reliability of the EV/K_2CO_3 composite material is contingent upon its cycling stability. An experimental study was conducted to assess the cyclic stability of the EV/K_2CO_3 composite material. The $EVPC_{40}$ sample was chosen for investigation, with two humidity test protocols established, with one involving six hydration–dehydration cycles at low humidity (30 °C and 29% RH) and the other consisting of sixteen cycles under high humidity conditions (30 °C and 60% RH). These tests were carried out using a CHTC apparatus, and, prior to these tests, all samples were subjected to preconditioning at 150 °C for a duration of 6 h in order to establish a stable baseline. The initial masses of the samples were approximately 22 mg for the low-humidity trials and approximately 65 mg for the high-humidity experiments. The objective of this series of tests was to assess the performance consistency and durability of the EV/K_2CO_3 composite material under multiple hydration–dehydration cycles.

2.6. Data Processing

The reaction rate of the thermochemical processes of the EV/K_2CO_3 composite materials can be determined via data processing of the results obtained from the CTHC experiments or STA tests. The relative reaction rate is expressed as $d\alpha/d\tau$ (min^{-1}), which corresponds to the derivative of the material conversion, α, as a function of time, τ. As shown in Equation (1), α can be calculated directly using the results of the sorption or desorption experiments

$$\alpha = \frac{m_{\tau_0} - m_\tau}{m_{\tau_0} - m_{\tau_\infty}} \tag{1}$$

where m_{τ_0} and m_{τ_∞} represent the initial and the final masses of the EV/K_2CO_3 composite materials during the sorption or desorption processes, respectively, and m_τ represents the mass of the EV/K_2CO_3 composite materials at the reaction time τ.

The relative reaction rate is meaningful only when one sorbent has the same water uptake. Therefore, the absolute sorption (desorption) rate, $SR(DSR)$, is introduced to compare different sorbents with different water uptakes, and the definition is shown in Equation (2):

$$SR(DSR) = \frac{m_{\tau_2} - m_{\tau_1}}{\tau_2 - \tau_1} \tag{2}$$

where m_{τ_1} and m_{τ_2} represent the masses of the EV/K_2CO_3 composite materials at the reaction times τ_1 and τ_2 during the sorption or desorption processes, respectively.

The reaction enthalpy of the desorption process can be determined by processing the data of the DSC results. On the DSC curve, the enthalpy of the reaction corresponds to the DSC peak area, which can be obtained by integrating the curve using Equation (3)

$$\Delta_r H = \int_{\tau_0}^{\tau_\infty} Q_\tau d\tau \tag{3}$$

where τ_0 and τ_∞ represent the initial and final times of the reaction, respectively, and Q_τ represents the heat flux of the EV/K_2CO_3 composite materials at the reaction time τ.

3. Results and Discussion

3.1. SEM Images and Salt Contents

Based on the preparation procedure illustrated in Figure 1, EV/K_2CO_3 composite materials were fabricated with different salt contents. The corresponding salt content and

bulk density values are presented in Table 1. The data clearly indicates that an increase in the concentration of the impregnation K_2CO_3 solution results in a corresponding rise in the salt content of the EV/K_2CO_3 composite materials, as well as an increase in bulk density. This finding suggests that a higher concentration of the impregnation solution facilitates the filling of a greater amount of K_2CO_3 salt into the voids of the EV.

Table 1. Salt content and bulk density of EV, EV/K_2CO_3 composites, and K_2CO_3.

Samples	EV	$EVPC_{10}$	$EVPC_{20}$	$EVPC_{30}$	$EVPC_{40}$	K_2CO_3
Salt content, θ (%)	0	31.1	43.1	64.4	67.4	100
Bulk density, ρc (kg/m^3)	128 [1]	181	216	327	353	2428 [2]

[1] Taken from ref. [23]. [2] Taken from ref. [28].

To further observe the microstructure of EV/K_2CO_3 composite materials under varying salt contents, SEM images were acquired, as depicted in Figure 2. It is evident that an augmentation in salt content leads to an escalation in the surface roughness of the EV/K_2CO_3 composite material. This phenomenon can be attributed to a higher proportion of K_2CO_3 salt occupying the surface of the EV layer. In the case of $EVPC_{40}$, the K_2CO_3 salt nearly entirely covers the surface of the EV layer, forming a honeycomb-like layer with numerous macropores and mesopores. The multitude of channels and pore structures present in the material offer a wide range of attachment sites for salt particles, effectively preventing their aggregation and promoting uniform dispersion. Additionally, the distinctive capillary forces between pores can adsorb and stabilize salt particles, thereby enhancing the homogeneous distribution of salt particles within the pores. Therefore, the incorporation of EV as a matrix material not only effectively disperses salt particles, thus reducing particle aggregation, but also greatly increases the specific surface area of the composite material, leading to improved overall performance.

3.2. Sorption Properties

Figure 3 illustrates the sorption kinetics curves of dried EV and EV/K_2CO_3 composite materials with varying salt content at 30 °C and 60% RH. It can be observed that the equilibrium water uptake of EV is merely 0.04 g/g. However, the inclusion of K_2CO_3 salt particles significantly increases the water uptake of EV/K_2CO_3 composite materials. The known theoretical chemical adsorption capacity of K_2CO_3 for water vapor is 0.20 g/g, while the equilibrium water uptake (the time required to reach sorption equilibrium) for $EVPV_{10}$, $EVPC_{20}$, $EVPC_{30}$, and $EVPC_{40}$ is 0.32 g/g (5.0 h), 0.42 g/g (7.0 h), 0.63 g/g (14.5 h), and 0.68 g/g (16 h), respectively. It is worth noting that the equilibrium water uptake of the EVPC40 sample is 3.4 times the theoretical chemical adsorption capacity of pure K_2CO_3 salt. The increase in K_2CO_3 salt content is found to positively correlate with the equilibrium water uptake of EV/K_2CO_3 composite materials, suggesting the significant influence of salt content on the sorption process. This observation further suggests the presence of solution absorption in addition to physical and chemical adsorption in EV/K_2CO_3 composite materials, as supported by the findings of Shkatulov et al. [26]. Therefore, upon attaining sorption equilibrium, the EV/K_2CO_3 composite materials exhibit the presence of K_2CO_3 within the interstices of EV in a solute form. The quantified values for the physical adsorption of EV ($x_{ad,EV}$), the chemical adsorption of K_2CO_3 ($x_{ad,salt}$), the absorption of K_2CO_3 solution ($x_{ab,salt}$), and the mass concentration of the K_2CO_3 salt solution (c_{salt}) at the sorption equilibrium are listed in Table 2, employing Equations (4)–(7).

$$x_{ad,EV} = (1 - \theta) \cdot x_{w,EV} \quad (4)$$

$$x_{ad,salt} = \theta \cdot x_{cs,salt} \quad (5)$$

$$x_{ab,salt} = x_{w,EVPC} - x_{ad,EV} - x_{ad,salt} \quad (6)$$

$$c_{\text{salt}} = \frac{\theta}{\theta + x_{\text{w,EVPC}} - (1-\theta) \cdot x_{\text{w,EV}}} \times 100\% \quad (7)$$

where $x_{\text{w,EV}}$ and $x_{\text{w,EVPC}}$ represent the total water uptake of EV and EV/K_2CO_3 composite materials, respectively. The theoretical saturation chemical adsorption capacity of K_2CO_3 is denoted as $x_{\text{cs,salt}}$, with a specific value of 0.20 g/g. The parameter θ corresponds to the salt content of the material, and its respective values can be obtained from Table 1.

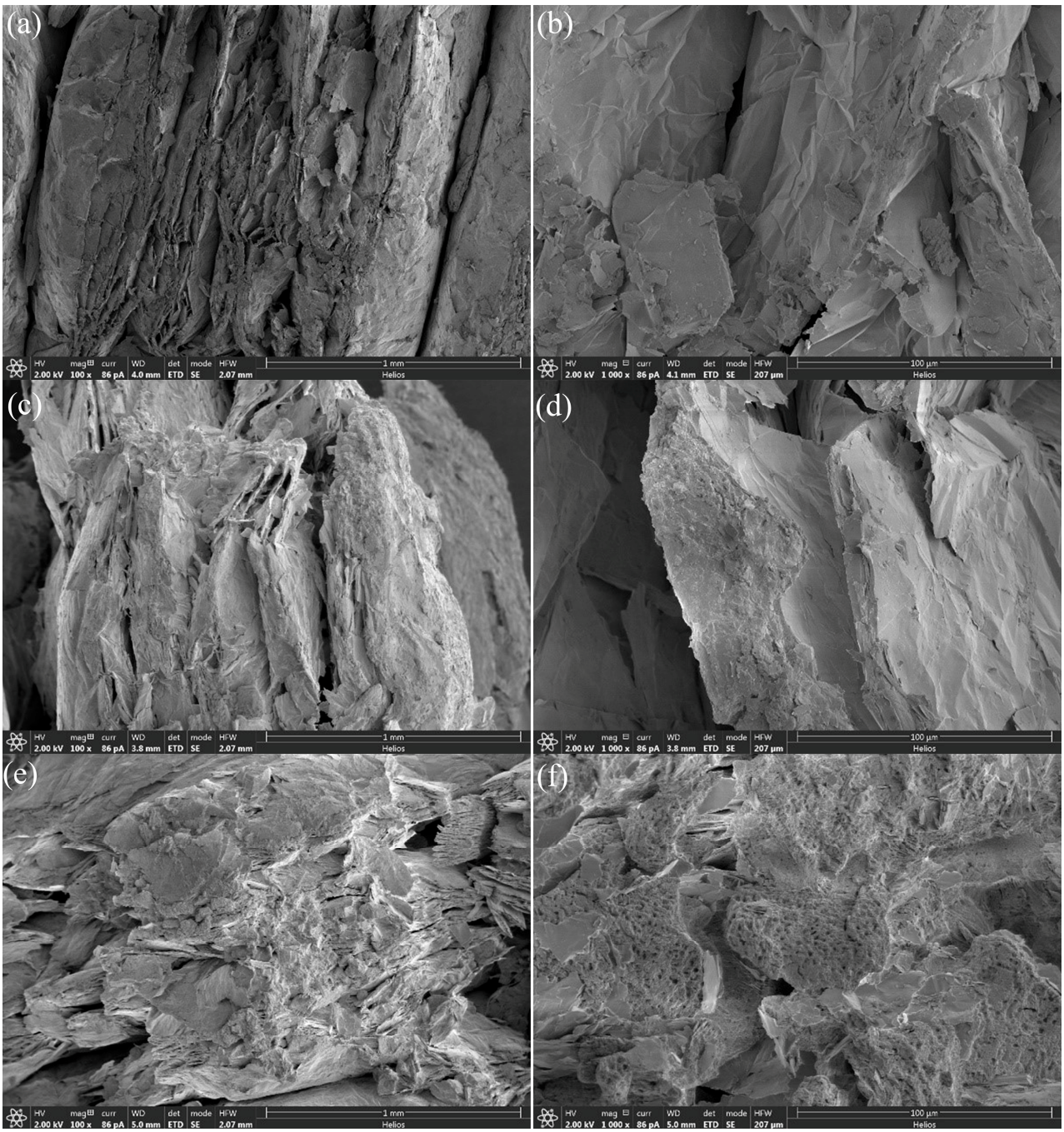

Figure 2. SEM images of the dried EV and EV/K_2CO_3 composites: (**a**) 100 and (**b**) 1000 times magnified SEM images of EV; (**c**) 100 and (**d**) 1000 times magnified SEM images of $EVPC_{20}$; (**e**) 100 and (**f**) 1000 times magnified SEM images of $EVPC_{40}$.

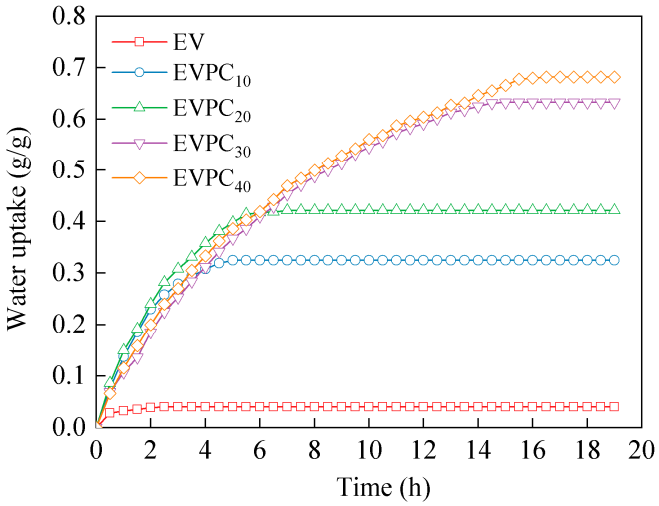

Figure 3. Sorption kinetic curves of EV and EV/K_2CO_3 composites at 30 °C and 60% RH.

Table 2. Evaluation of water uptake behavior of EV/K_2CO_3 composites.

Samples	$EVPC_{10}$	$EVPC_{20}$	$EVPC_{30}$	$EVPC_{40}$
$x_{ad,EV}$ (g/g)	0.03	0.02	0.02	0.02
$x_{ad,salt}$ (g/g)	0.07	0.11	0.13	0.13
$x_{ab,salt}$ (g/g)	0.22	0.29	0.48	0.53
$x_{w,EVPC}$ (g/g)	0.32	0.42	0.63	0.68
c_{salt} (%)	51.7	52.4	51.1	50.2

Based on the data presented in Table 2, it is apparent that the water uptake of the EV/K_2CO_3 composite materials is predominantly attributed to chemical adsorption and solution absorption processes, accounting for approximately 19.1% to 20.2% and 71.8% to 78.6% of the total, respectively. The physical adsorption of EV plays a minor role in the overall water uptake of the EV/K_2CO_3 composite materials, constituting approximately 2.9% to 9.4%. Moreover, the influence of physical adsorption decreases as the salt content increases. The mass concentrations of the salt solutions for the four samples obtained at sorption equilibrium are 51.7%, 52.4%, 51.1%, and 50.2%, respectively. These values are closely aligned with the mass concentration of a saturated K_2CO_3 solution at the same temperature (30 °C), which is 53.1%. This observation implies that the presence of EV, serving as the substrate for K_2CO_3 salt, does not have a substantial impact on the sorption equilibrium of the reaction salt.

The aforementioned findings were acquired at a relative humidity of 60%. Furthermore, experiments were conducted to assess the sorption capabilities of the $EVPC_{40}$ composite material at various relative humidities, while keeping the temperature constant at 30 °C. The outcomes are depicted in Figure 4. When the relative humidity falls below 43%, the water uptake of the $EVPC_{40}$ composite material remains consistently at 0.12~0.13 g/g, which aligns with its theoretical chemical adsorption capacity (0.13 g/g). This indicates that no deliquescence occurs at this point. In contrast, when the relative humidity exceeds 43%, the water uptake experiences a rapid escalation, which further amplifies with subsequent increases in relative humidity. This observation suggests that the composite material undergoes deliquescence, thereby exhibiting the phenomenon of solution absorption. Additionally, it implies that the EV, acting as the substrate for the K_2CO_3 salt, does not significantly influence the critical relative humidity of the reaction salt.

In summary, the EV/K_2CO_3 composite material, wherein EV serves as the porous substrate, effectively preserves the sorption properties exhibited by pure K_2CO_3 salt. Furthermore, no substantial leakage was observed after all samples reached sorption equilibrium. This indicates that the EV/K_2CO_3 composite material not only significantly increases the total water uptake but also effectively accommodates the salt solution formed due to

deliquescence and excessive hydration of K_2CO_3 salt, thereby mitigating material loss and enhancing the stability of utilizing TCES materials.

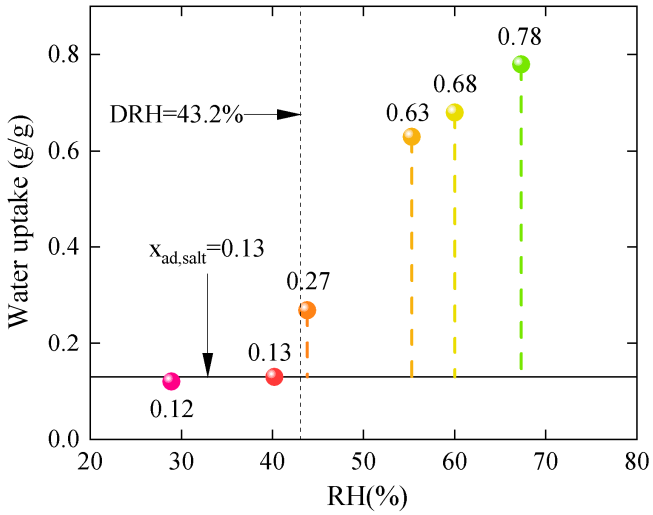

Figure 4. The equilibrium water uptake of the EV/K_2CO_3 composite under different RH conditions, with a consistent temperature of 30 °C.

The EV/K_2CO_3 composite materials exhibit similar sorption properties as pure K_2CO_3 salt, allowing for the utilization of conventional analytical techniques employed for pure K_2CO_3 salt in the analysis of the EV/K_2CO_3 composite materials. Consequently, the sorption process of the EV/K_2CO_3 composite materials can be delineated into two distinct stages: adsorption and absorption.

The first sorption stage:

$$EV + K_2CO_3(s) + 1.5H_2O(g) \rightarrow EV + K_2CO_3 \cdot 1.5H_2O\ (s) + Heat \quad (8)$$

The second sorption stage:

$$EV + K_2CO_3 \cdot 1.5H_2O\ (s) + nH_2O(g) \rightarrow EV + K_2CO_3\ solution + Heat \quad (9)$$

where *n* is a constant that can be calculated via conversion using the salt concentration at the final sorption equilibrium state of EV/K_2CO_3 composite materials. In this study, the value of n ranges approximately between 5.5 and 6.1.

The sorption rates of the two sorption stages of EV/K_2CO_3 composite materials are illustrated in Figure 5. It can be observed that the average sorption rates for the first and second stages are 2.06 × 10^{-3} g/g·min^{-1} and 0.72 × 10^{-3} g/g·min^{-1}, respectively. The average sorption rate of the first stage is approximately 2.4 to 3.3 times that of the second stage. This disparity can be attributed to the greater sorption energy associated with crystalline water bonded in chemical form compared to structural water and free water. Moreover, the salt content has a certain influence on the average sorption rates of these two stages. The average sorption rate of the first stage initially increases and then decreases with an increase in salt content. This suggests that the augmentation in salt content could potentially result in heightened resistance to mass transfer, potentially attributable to the occupation of pore volume by salt particles, as corroborated by the investigation conducted by Michel et al. [29]. The average sorption rate of the second stage slightly decreases with an increase in salt content, but the variation is not significant. Therefore, although increasing the salt content can enhance the water uptake of the composite materials, it may also impede the sorption rate due to an elevation in mass transfer resistance.

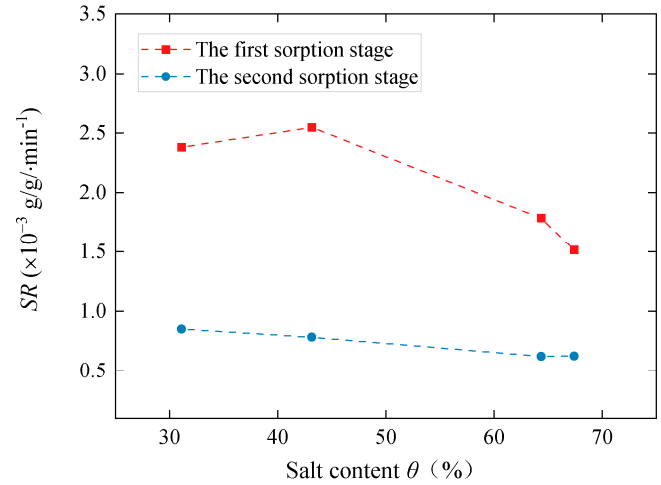

Figure 5. Average sorption rate versus salt content for the EV/K_2CO_3 composites.

3.3. Desorption Properties

The desorption process of potassium carbonate hydrate salt can be utilized for efficient thermal energy storage involving a single-step conversion between $K_2CO_3 \cdot 1.5H_2O$ and K_2CO_3 [30]. However, the desorption process of EV exhibits a more complex series of two to three steps, as shown in Figure 6. As the temperature increases, the adsorbed water in EV gradually evaporates, resulting in three distinct peaks during the desorption process at temperatures of 32.9 °C, 70 °C, and 133.4 °C, respectively. The combined mass loss of the first two mass plateaus accounts for approximately 90% of the total mass loss. In order to examine the potential impact of the EV substrate on the desorption performance of EV/K_2CO_3 composite materials, desorption experiments were conducted on composite materials with varying salt contents, considering the unique desorption process of EV in comparison to pure $K_2CO_3 \cdot 1.5H_2O$.

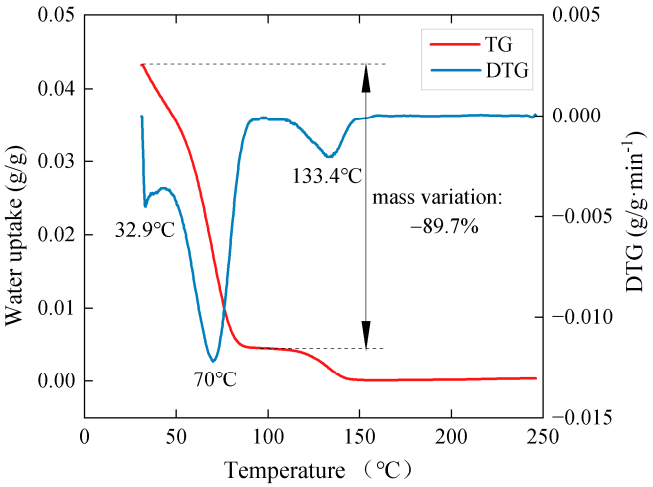

Figure 6. TG test outcomes of EV at the heating rate of 10 K/min.

Figure 7 presents the TG test outcomes of the EV/K_2CO_3 composite materials attaining sorption equilibrium under initial conditions of 30 °C and 60% RH. It can be observed that the desorption process of the EV/K_2CO_3 composite materials encompasses three to four steps, and with an increase in salt content, the temperature peaks of each mass plateau generally shift to the right. This indicates that the incorporation of the EV porous matrix complicates the dehydration process, which can be attributed to the complex structure of EV or possibly to the heating rate. At higher heating rates, the desorption process of salt hydrates may result in melting, causing localized peaks [31].

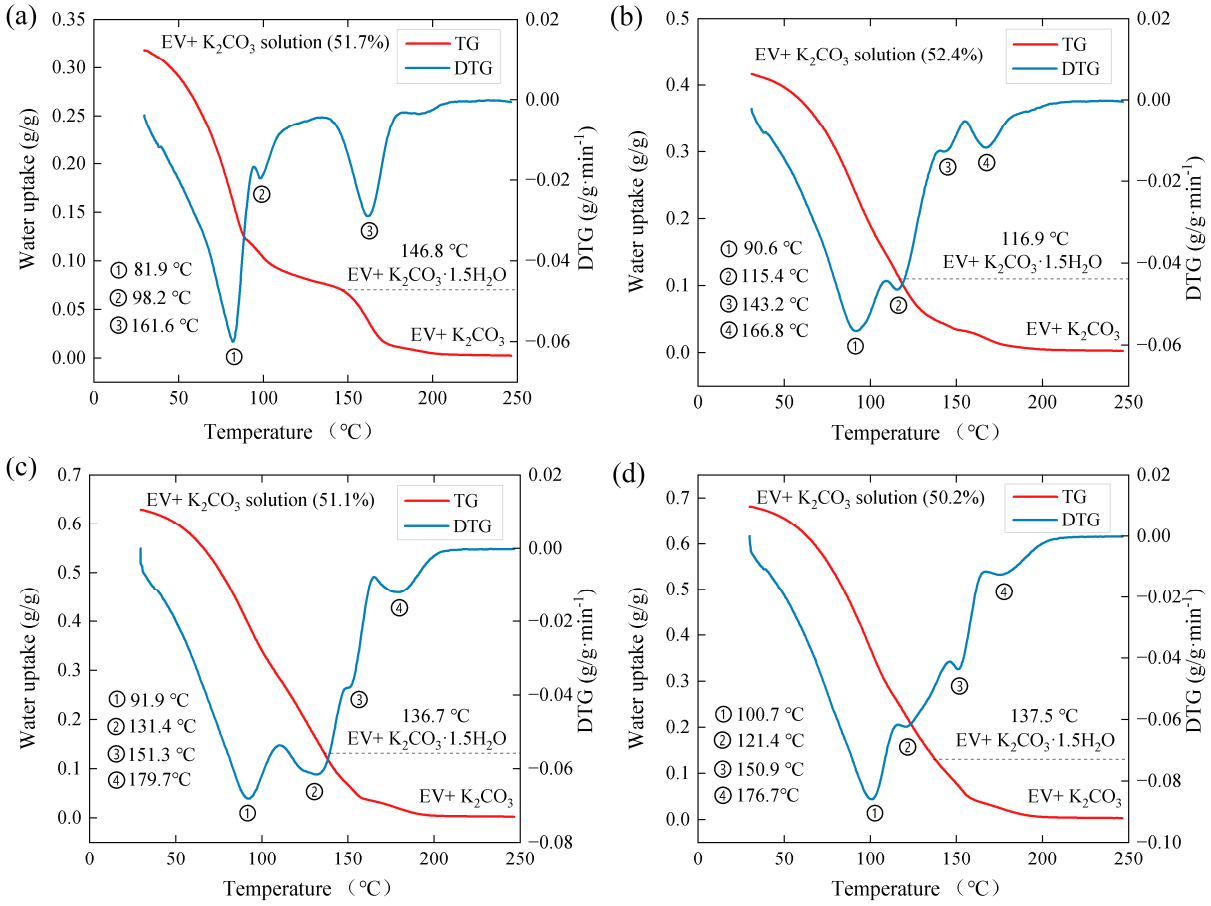

Figure 7. TG test outcomes of EV/K_2CO_3 composites at the heating rate of 10 K/min: (**a**) $EVPC_{10}$; (**b**) $EVPC_{20}$; (**c**) $EVPC_{30}$; (**d**) $EVPC_{40}$.

The boundary line for the desorption process of the EV/K_2CO_3 composite materials is taken as EV + K_2CO_3·1.5H_2O(s), represented by the horizontal dashed line in Figure 7a–d. The initial two steps primarily involve the conversion from EV + K_2CO_3 solution to EV + K_2CO_3·1.5H_2O(s), while the subsequent one or two steps mainly involve the conversion from EV + K_2CO_3·1.5H_2O(s) to EV + K_2CO_3(s). Consequently, these two conversion processes can be described by the two desorption stages outlined in Equations (10) and (11).

The first desorption stage:

$$\mathrm{EV} + \mathrm{K_2CO_3\ solution} + \mathrm{Heat} \rightarrow \mathrm{EV} + \mathrm{K_2CO_3 \cdot 1.5H_2O\ (s)} + m\mathrm{H_2O(g)} \quad (10)$$

The second desorption stage:

$$\mathrm{EV} + \mathrm{K_2CO_3 \cdot 1.5H_2O\ (s)} + \mathrm{Heat} \rightarrow \mathrm{EV} + \mathrm{K_2CO_3(s)} + 1.5\mathrm{H_2O(g)} \quad (11)$$

According to Equation (2), the average desorption rates of EV/K_2CO_3 composite materials with different salt contents can be determined for the two desorption stages outlined in Equations (10) and (11), as depicted in Figure 8. It can be seen that the average desorption rates for these stages are 3.60×10^{-2} g/g·min^{-1} and 1.05×10^{-2} g/g·min^{-1}, respectively. Notably, the average desorption rate of the first desorption stage is approximately three to four times that of the second desorption stage, owing to the higher activation energy required for the dehydration of chemically bound crystalline water in comparison to structural water and free water. Moreover, the salt content has a discernible influence on the average desorption rates of the two desorption states in EV/K_2CO_3 composite materials. Specifically, as the salt content increases, the average desorption rates exhibit a

corresponding increase. Consequently, increasing the salt content proves advantageous for enhancing the desorption rate of EV/K_2CO_3 composite materials, which is significantly faster compared to the sorption process. Therefore, in practical applications of salt hydrates, the sorption process typically acts as the primary limiting factor.

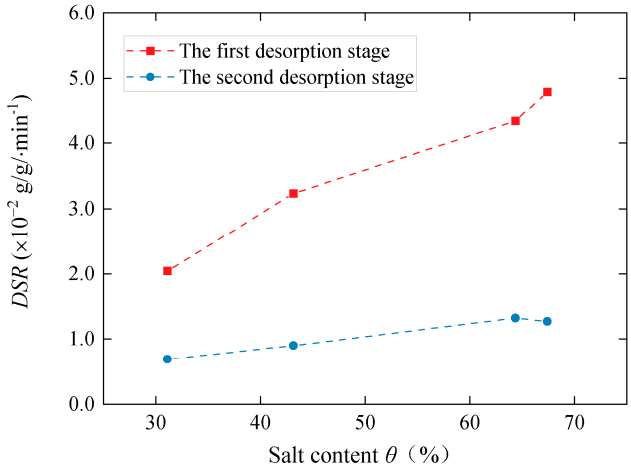

Figure 8. Average desorption rate versus salt content for the EV/K_2CO_3 composites.

3.4. Cycle Stability

The assessment of the reliability and repeatability of the sorption properties of the EV/K_2CO_3 composite material relies on the consistency and stability of the data. Figure 9 illustrates the variation in water uptake of $EVPC_{40}$ composite material during six hydration–dehydration cycles in the case of RH lower than DRH (i.e., 30 °C and 29% RH), starting with an initial mass of approximately 22 mg. Throughout these cycles, the equilibrium water uptake remained constant within a narrow range of 0.120–0.124 g/g, with an average of 0.122 g/g and a minimal standard deviation of approximately 0.001 g/g. This observation highlights the consistent maintenance of sorption levels within a narrow range, despite minor inherent variations in repeated experiments. This indicates strong data consistency and suggests that the EV/K_2CO_3 composite material demonstrates a high level of stability and repeatability in its sorption performance under conditions of low humidity.

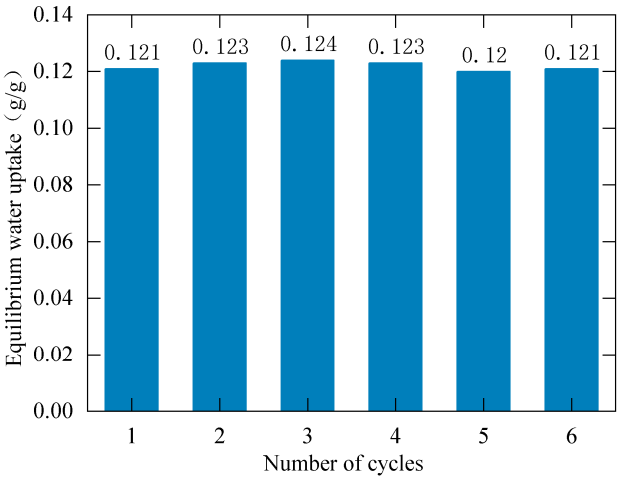

Figure 9. Equilibrium water uptake of the $EVPC_{40}$ composite material during six cycles in the case of RH lower than DRH.

Figure 10 presents the mass change of the $EVPC_{40}$ composite material during the 16 hydration-dehydration cycles in the case of RH higher than DRH (i.e., 30 °C and 60%

RH). The initial mass of the sample following the first drying process was recorded at 65.53 mg, and subsequent measurements after 16 cycles of hydration–dehydration revealed a mass of 65.42 mg, indicating minimal variation in mass before and after the cycles. The average sample mass over the course of the 16 cycles remained constant at 65.42 mg, with a deviation of no more than 0.5% between the maximum (65.53 mg) and minimum (65.32 mg) values. These findings suggest that the EV/K_2CO_3 composite material experienced no solution leakage after 16 cycles, demonstrating strong cycling stability and reinforcing its potential for reliable performance in practical applications.

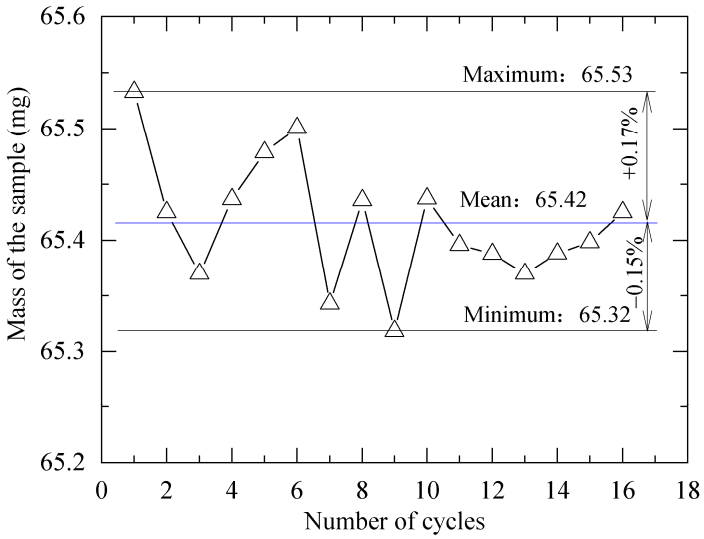

Figure 10. Sample mass of the $EVPC_{40}$ composite material during 16 cycles in the case of RH higher than DRH.

3.5. Thermal Energy Storage Properties

The MESD and the VESD are two important parameters for evaluating the heat storage efficiency of TCES systems. The MESD of EV/K_2CO_3 composite materials ($Q_{m,EVPC}$) includes three components, the physical adsorption heat of EV ($Q_{ad,EV}$), the chemical adsorption heat of K_2CO_3 salt ($Q_{ad,salt}$), and the absorption heat of K_2CO_3 solution ($Q_{ab,salt}$), as illustrated in Equation (12). The VESD of EV/K_2CO_3 composite materials ($Q_{V,EVPC}$) can be obtained by converting the MESD using Equation (13).

$$Q_{m,EVPC} = Q_{ad,EV} + Q_{ad,salt} + Q_{ab,salt} \quad (12)$$

$$Q_{V,EVPC} = \rho_c \cdot Q_{m,EVPC} \quad (13)$$

where ρ_c represents the mass density of the EV/K_2CO_3 composite materials, which can be obtained from Table 1.

The DSC experimental curve, obtained through the utilization of DSC for thermal analysis of the samples, is shown in Figure A1. The characteristics observed in the DSC data exhibit similarities to those depicted in the DTG curves of Figures 6 and 7. By integrating the DSC curve, the desorption heat of the EV/K_2CO_3 composite materials can be determined, as presented in Table 3. It is evident that the desorption heat of the EV/K_2CO_3 composite materials rises with the augmentation of salt content. Among them, the $EVPC_{40}$ sample exhibits a desorption heat of 1633.6 kg/kg.

Table 3. Dehydration heat of EV and EV/K_2CO_3 composites at the heating rate of 10 K/min.

Samples	EV	$EVPC_{10}$	$EVPC_{20}$	$EVPC_{30}$	$EVPC_{40}$
Desorption heat (kJ/kg)	81.6	818.0	1091.3	1572.0	1633.6

Because the sorption process of salt hydrates can be considered a reversible process of desorption, the sorption heat is equal to the desorption heat. By utilizing Equations (14)–(16), it is possible to indirectly ascertain the physical adsorption heat of EV, the chemical adsorption heat of K_2CO_3 salt, and the absorption heat of the K_2CO_3 solution.

$$Q_{ad,EV} = (1 - \theta) \cdot Q_{m,EV} \quad (14)$$

$$Q_{ad,salt} = \theta \cdot Q_{cs,salt} \quad (15)$$

$$Q_{ab,salt} = Q_{m,EVPC} - Q_{ad,EV} - Q_{ad,salt} \quad (16)$$

Figure 11 depicts the variations in the MESD and VESD of EV/K_2CO_3 composite materials as a function of salt content. It is evident that both the MESD and VESD of EV/K_2CO_3 composites exhibit an upward trend with increasing salt content. This observation suggests that augmenting the salt content confers advantages in enhancing the heat storage performance of the material and serves as a crucial determinant of the thermal energy storage density. Furthermore, the MESD of EV/K_2CO_3 composites exceeds that of pure K_2CO_3 salt gas–solid adsorption. This can be predominantly ascribed to the presence of EV, which possesses the ability to accommodate the salt solution generated from salt deliquescence and excessive hydration without any leakage, effectively utilizing the heat absorbed by the solution in EV/K_2CO_3 composite materials. This portion of heat accounts for approximately 66 to 69% of the total heat. Among the various materials examined, the $EVPC_{40}$ composite material demonstrates the highest heat storage density, as evidenced by its VESD of up to 160 kWh/m^3 and its MESD of 1633.6 kJ/kg. This MESD value is approximately 2.34 times that of pure K_2CO_3 salt (710 kJ/kg). This suggests that the utilization of EV/K_2CO_3 composite materials, in comparison to pure K_2CO_3 salt, can result in a cost reduction of approximately 57% for TCES materials under identical heat demand conditions. Thus, the inclusion of EV as a porous matrix in EV/K_2CO_3 composite materials presents a promising option for the advancement of TCES materials in forthcoming research.

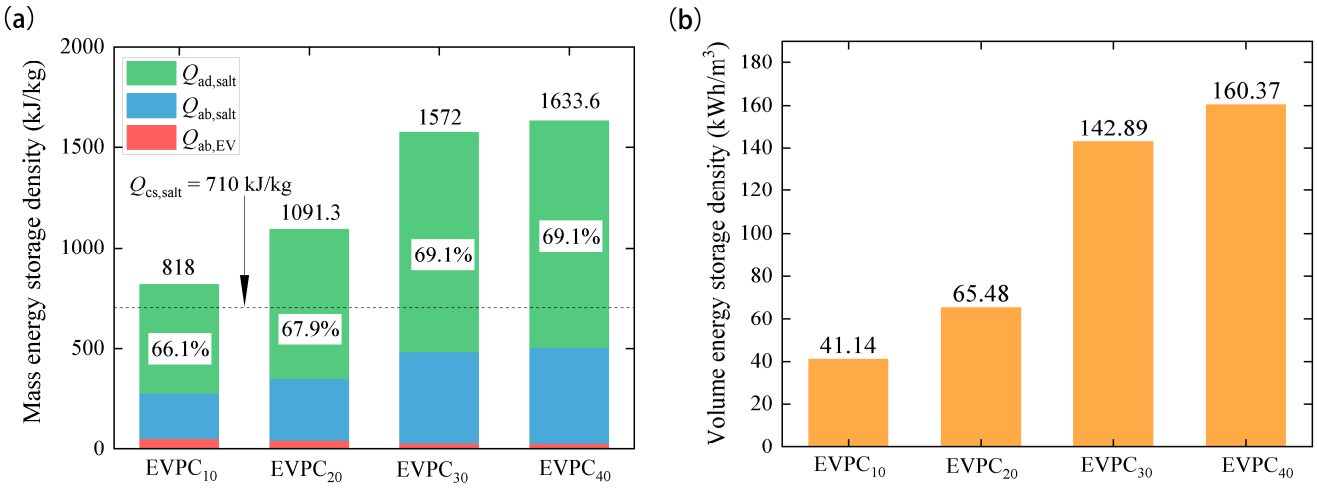

Figure 11. The (**a**) MESD and (**b**) VESD of the EV/K_2CO_3 composites with different salt content.

4. Conclusions

This study employed a solution impregnation method to fabricate EV/K_2CO_3 composite materials with varying salt content. The microscopic morphology of these composite materials was meticulously examined via SEM, while the sorption and desorption kinetics performances were rigorously investigated through CTHC experiments and STA testing. Furthermore, the MESD and VESD of the EV/K_2CO_3 composite materials were determined using the DSC analysis. The main conclusions are as follows.

In the context of EV/K_2CO_3 composite materials, the inclusion of EV has been found to have several beneficial effects. Firstly, the presence of EV effectively disperses salt

particles, mitigating their tendency to aggregate and promoting a larger specific surface area for the composite material. Importantly, this dispersion does not disrupt the sorption equilibrium or critical relative humidity of the reacting salt. Additionally, EV serves as a reservoir for the salt solution, effectively addressing the issue of solution leakage caused by deliquescence and excessive hydration of pure K_2CO_3 salt. This reservoir function significantly enhances the water uptake and stability of the composite material. Hence, EV demonstrates its appropriateness as a matrix material for K_2CO_3 and holds practical value and significant potential in TCES systems.

The salt content plays a crucial role in determining the performance of EV/K_2CO_3 composite materials. The water uptake of these composites surpasses the chemical adsorption capacity of pure K_2CO_3 salt, primarily attributed to the solution absorption of K_2CO_3. Notably, an increase in salt content directly correlates with higher water uptake. In the desorption process, increasing the salt content has been observed to positively influence the average desorption rate. Conversely, in the sorption process, elevating the salt content has been found to enhance the water uptake but concurrently increase the resistance to mass transfer, leading to a decrease in the average sorption rate. This indicates that the sorption process may serve as the primary limiting factor in its kinetic performance. Moreover, the MESD and VESD of EV/K_2CO_3 composite materials exhibit an upward trend with the augmentation of salt content. In terms of enhancing energy density, it is advisable to maximize the salt content of EV/K_2CO_3 composite materials while ensuring the absence of solution leakage.

Among the various EV/K_2CO_3 composite materials analyzed in this study, the $EVPC_{40}$ composite material, characterized by a salt content of 67.4% and operating conditions of 30 °C and 60%RH, is deemed to be the optimal TCES material. It exhibits a water uptake of 0.68 g/g, with MESD and VESD values of 1633.6 kJ/kg and 160 kWh/m^3, respectively. In terms of cost savings, employing EV/K_2CO_3 composite materials under identical heat demand conditions can result in a reduction of approximately 57% compared to the utilization of pure K_2CO_3 salt, thus establishing it as a highly promising TCES material.

The present study provides fundamental data and theoretical backing for the utilization and design of EV/K_2CO_3 composite materials in TCES systems. Future research efforts will focus on exploring the performance of EV/K_2CO_3 composite materials under diverse operational circumstances, as well as delving deeper into the relevant properties of EV/K_2CO_3 composite materials at both the reactor and system levels.

Author Contributions: Conceptualization, J.L. and Q.Z.; methodology, J.L.; software, J.L.; validation, J.L. and Q.Z.; formal analysis, J.L.; investigation, Q.Z. and H.H.; resources, J.L.; data curation, J.L. and Q.Z.; writing—original draft preparation, J.L.; writing—review and editing, Q.Z. and H.H.; visualization, J.L.; supervision, J.L. and Q.Z.; project administration, J.L.; funding acquisition, J.L. All authors have read and agreed to the published version of the manuscript.

Funding: This work was supported by the Changzhou Leading Innovative Talents Introduction and Cultivation Project (grant number KYZ23020035) and the High-level Talent Introduction Program of Changzhou University (grant number ZMF23020070).

Data Availability Statement: Data are contained within the article.

Conflicts of Interest: The authors declare that they have no known competing financial interests or personal relationships that could have appeared to influence the work reported in this paper.

Abbreviations

The following abbreviations are used in this manuscript.

Abbreviations

CTHC	constant temperature and humidity chamber
DRH	deliquescence relative humidity
DSC	differential scanning calorimetry
DSR	desorption rate
EV	expanded vermiculite
MESD	mass energy storage density
RH	relative humidity
SEM	scanning electron microscope
SR	sorption rate
STA	Simultaneous Thermal Analyzer
TCES	thermochemical energy storage
TCM	thermochemical material
TG	thermogravimetry
VESD	volumetric energy storage density

Nomenclature

m	masses of samples
Q	heat flux or sorption heat
x	water uptake of samples
c_{salt}	mass concentration of the K_2CO_3 salt solution

Greek Symbols

α	material conversion
θ	salt content
ρ	mass density
τ	reaction time

Subscripts

ab,salt	absorption of K_2CO_3 solution for EV/K_2CO_3 composites
ad,EV	physical adsorption of EV for EV/K_2CO_3 composites
ad,salt	chemical adsorption of K_2CO_3 for EV/K_2CO_3 composites
cs,salt	theoretical saturation chemical adsorption capacity of pure K_2CO_3
m,EVPC	sorption of EV/K_2CO_3 composites
w,EV	sorption of pure EV

Appendix A

The DSC measurement results of the EV and EV/K_2CO_3 composites at the heating rate of 10 K/min are shown in Figure A1.

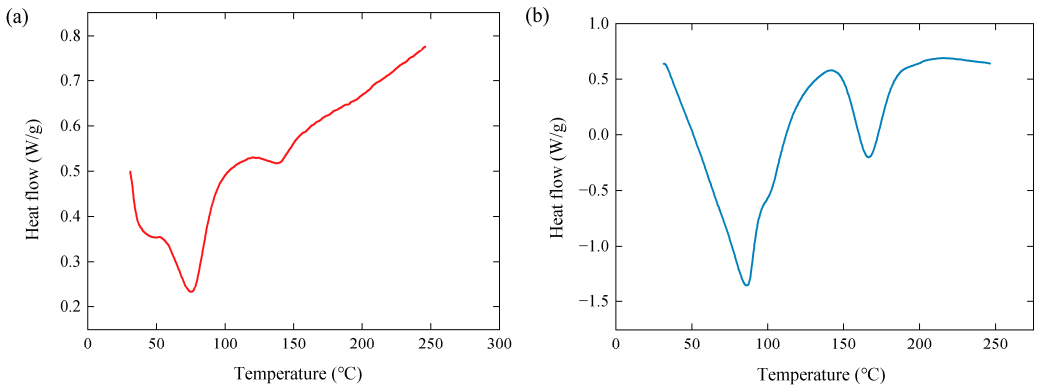

Figure A1. *Cont.*

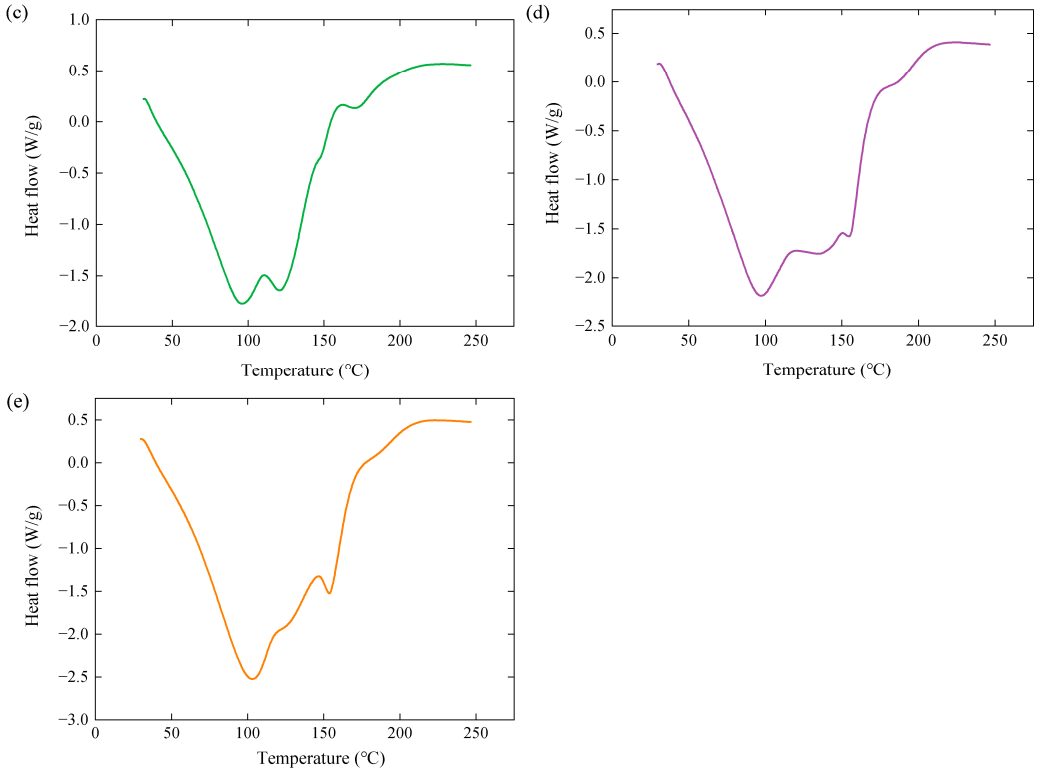

Figure A1. The DSC measurement results of the EV and EV/K_2CO_3 composites at the heating rate of 10 K/min: (**a**) EV; (**b**) $EVPC_{10}$; (**c**) $EVPC_{20}$; (**d**) $EVPC_{30}$; (**e**) $EVPC_{40}$.

References

1. Yan, T.; Wang, R.Z.; Li, T.X.; Wang, L.W.; Fred, I.T. A Review of Promising Candidate Reactions for Chemical Heat Storage. *Renew. Sustain. Energy Rev.* **2015**, *43*, 13–31. [CrossRef]
2. Lefebvre, D.; Tezel, F.H. A Review of Energy Storage Technologies with a Focus on Adsorption Thermal Energy Storage Processes for Heating Applications. *Renew. Sustain. Energy Rev.* **2017**, *67*, 116–125. [CrossRef]
3. Almendros-Ibáñez, J.A.; Fernández-Torrijos, M.; Díaz-Heras, M.; Belmonte, J.F.; Sobrino, C. A Review of Solar Thermal Energy Storage in Beds of Particles: Packed and Fluidized Beds. *Sol. Energy* **2019**, *192*, 193–237. [CrossRef]
4. Sullivan, G.; Griffiths, C.; Jewell, E.; Searle, J.; Elvins, J. Cycling Stability of Calcium-Impregnated Vermiculite in Open Reactor Used as a Thermochemical Storage Material. *Energies* **2023**, *16*, 7225. [CrossRef]
5. Shchegolkov, A.; Shchegolkov, A.; Demidova, A. The Use of Nanomodified Heat Storage Materials for Thermal Stabilization in the Engineering and Aerospace Industry as a Solution for Economy. *MATEC Web Conf.* **2018**, *224*, 03012. [CrossRef]
6. Shchegolkov, A.V.; Shchegolkov, A.V.; Galunin, E.V.; Popova, A.A.; Krivosheev, R.M.; Memetov, N.R.; Tkachev, A.G. Graphene-Modified Heat-Accumulating Materials and Aspects of Their Application in Thermotherapy and Biotechnologies. *Nano Hybrids Compos.* **2017**, *13*, 21–25. [CrossRef]
7. Yan, T.; Zhang, H. A Critical Review of Salt Hydrates as Thermochemical Sorption Heat Storage Materials: Thermophysical Properties and Reaction Kinetics. *Sol. Energy* **2022**, *242*, 157–183. [CrossRef]
8. Hua, W.; Yan, H.; Zhang, X.; Xu, X.; Zhang, L.; Shi, Y. Review of Salt Hydrates-Based Thermochemical Adsorption Thermal Storage Technologies. *J. Energy Storage* **2022**, *56*, 106158. [CrossRef]
9. Mohapatra, D.; Nandanavanam, J. Salt in Matrix for Thermochemical Energy Storage—A Review. *Mater. Today Proc.* **2023**, *72*, 27–33. [CrossRef]
10. ElBahloul, A.A.; Zeidan, E.-S.B.; El-Sharkawy, I.I.; Hamed, A.M.; Radwan, A. Recent Advances in Multistage Sorption Thermal Energy Storage Systems. *J. Energy Storage* **2022**, *45*, 103683. [CrossRef]
11. Fumey, B.; Weber, R.; Baldini, L. Sorption Based Long-Term Thermal Energy Storage—Process Classification and Analysis of Performance Limitations: A Review. *Renew. Sustain. Energy Rev.* **2019**, *111*, 57–74. [CrossRef]
12. Scapino, L.; Zondag, H.A.; Van Bael, J.; Diriken, J.; Rindt, C.C.M. Sorption Heat Storage for Long-Term Low-Temperature Applications: A Review on the Advancements at Material and Prototype Scale. *Appl. Energy* **2017**, *190*, 920–948. [CrossRef]
13. Aydin, D.; Casey, S.P.; Riffat, S. The Latest Advancements on Thermochemical Heat Storage Systems. *Renew. Sustain. Energy Rev.* **2015**, *41*, 356–367. [CrossRef]
14. Lin, J.; Zhao, Q.; Huang, H.; Mao, H.; Liu, Y.; Xiao, Y. Applications of Low-Temperature Thermochemical Energy Storage Systems for Salt Hydrates Based on Material Classification: A Review. *Sol. Energy* **2021**, *214*, 149–178. [CrossRef]

15. Donkers, P.A.J.; Sögütoglu, L.C.; Huinink, H.P.; Fischer, H.R.; Adan, O.C.G. A Review of Salt Hydrates for Seasonal Heat Storage in Domestic Applications. *Appl. Energy* **2017**, *199*, 45–68. [CrossRef]
16. Stanish, M.; Perlmutter, D. Kinetics and Transport Effects in the Dehydration of Crystalline Potassium Carbonate Hydrate. *AIChE J.* **1983**, *29*, 806–812. [CrossRef]
17. Deshpande, D.A.; Ghormare, K.R.; Deshpande, N.D.; Tankhiwale, A.V. Dehydration of Crystalline K_2CO_3·1.5 H_2O. *Thermochim. Acta* **1983**, *66*, 255–265. [CrossRef]
18. Sögütoglu, L.C.; Donkers, P.A.J.; Fischer, H.R.; Huinink, H.P.; Adan, O.C.G. In-Depth Investigation of Thermochemical Performance in a Heat Battery: Cyclic Analysis of K_2CO_3, $MgCl_2$ and Na_2S. *Appl. Energy* **2018**, *215*, 159–173. [CrossRef]
19. Zhao, Q.; Lin, J.; Huang, H.; Wu, Q.; Shen, Y.; Xiao, Y. Optimization of Thermochemical Energy Storage Systems Based on Hydrated Salts: A Review. *Energy Build.* **2021**, *244*, 111035. [CrossRef]
20. Aydin, D.; Casey, S.P.; Chen, X.; Riffat, S. Novel "Open-Sorption Pipe" Reactor for Solar Thermal Energy Storage. *Energy Convers. Manag.* **2016**, *121*, 321–334. [CrossRef]
21. Casey, S.P.; Elvins, J.; Riffat, S.; Robinson, A. Salt Impregnated Desiccant Matrices for 'Open' Thermochemical Energy Storage—Selection, Synthesis and Characterisation of Candidate Materials. *Energy Build.* **2014**, *84*, 412–425. [CrossRef]
22. Zhang, Y.; Wang, R.; Li, T.; Zhao, Y. Thermochemical Characterizations of Novel Vermiculite-LiCl Composite Sorbents for Low-Temperature Heat Storage. *Energies* **2016**, *9*, 854. [CrossRef]
23. Zhang, Y.N.; Wang, R.Z.; Zhao, Y.J.; Li, T.X.; Riffat, S.B.; Wajid, N.M. Development and Thermochemical Characterizations of Vermiculite/$SrBr_2$ Composite Sorbents for Low-Temperature Heat Storage. *Energy* **2016**, *115*, 120–128. [CrossRef]
24. Zou, D.; Yue, X.; He, T.; Ding, J.; Ba, D. Experimental Research on the Preparation of K_2CO_3/Expanded Vermiculite Composite Energy Storage Material. *Materials* **2022**, *15*, 3702. [CrossRef] [PubMed]
25. Fisher, R.; Ding, Y.; Sciacovelli, A. Hydration Kinetics of K_2CO_3, $MgCl_2$ and Vermiculite-Based Composites in View of Low-Temperature Thermochemical Energy Storage. *J. Energy Storage* **2021**, *38*, 102561. [CrossRef]
26. Shkatulov, A.I.; Houben, J.; Fischer, H.; Huinink, H.P. Stabilization of K_2CO_3 in Vermiculite for Thermochemical Energy Storage. *Renew. Energy* **2020**, *150*, 990–1000. [CrossRef]
27. Greenspan, L. Humidity Fixed Points of Binary Saturated Aqueous Solutions. *J. Res. Natl. Bur. Stand. Sect. A Phys. Chem.* **1977**, *81 A*, 89–96. [CrossRef]
28. Perry, D.L. *Handbook of Inorganic Compounds*; CRC Press: Boca Raton, FL, USA, 2016; ISBN 978-0-429-13036-6.
29. Michel, B.; Mazet, N.; Mauran, S.; Stitou, D.; Xu, J. Thermochemical Process for Seasonal Storage of Solar Energy: Characterization and Modeling of a High Density Reactive Bed. *Energy* **2012**, *47*, 553–563. [CrossRef]
30. Mazur, N.; Huinink, H.; Borm, B.; Sansota, S.; Fischer, H.; Adan, O. Thermodynamic Analysis of Dehydration of K_2CO_3·1.5H_2O. *Thermochim. Acta* **2022**, *715*, 179286. [CrossRef]
31. Yan, T.S.; Li, T.X.; Xu, J.X.; Chao, J.W. Understanding the Transition Process of Phase Change and Dehydration Reaction of Salt Hydrate for Thermal Energy Storage. *Appl. Therm. Eng.* **2020**, *166*, 114655. [CrossRef]

Disclaimer/Publisher's Note: The statements, opinions and data contained in all publications are solely those of the individual author(s) and contributor(s) and not of MDPI and/or the editor(s). MDPI and/or the editor(s) disclaim responsibility for any injury to people or property resulting from any ideas, methods, instructions or products referred to in the content.